

# **A fast focus measure for video display inspection**

D. M. Tsai and C. C. Chou

Machine Vision Lab.

Department of Industrial Engineering and Management

Yuan-Ze University, Chung-Li, Taiwan, R.O.C.

E-mail: [iedmtsai@saturn.yzu.edu.tw](mailto:iedmtsai@saturn.yzu.edu.tw)

## **Abstract**

In this paper we propose a robust and computationally fast focus measure for Cathode Ray Tubes (CRTs) found in TVs and computer and video monitors. The focus measure is represented by the area ratio of a predetermined object pattern in the test image of a fixed size, which will get larger as the degree of defocus increases. The area ratio is calculated using a simple, straightforward moment-preserving method. On-line, real-time application of focus adjustment can be realized with the proposed method.

*Keywords:* Automatic inspection; Focus measure; CRT focus; Moment preserving

## 1. Introduction

In this study we propose a robust and computationally efficient focus measure for color Cathode Ray Tubes (CRTs) found in TVs and computer and video monitors. The conventional procedure for the focus adjustment in the production line is generally carried out with human inspectors. The individual viewers are subjective to the focus quality on the screen, and their performance will degrade over time. It is impossible to adjust the focus to a fixed value, because every CRT is individual (Anttila and Tolmunen 1997). Therefore, the best focus quality must be found separately for each tube. In a manufacturing environment, rapid adjustment of CRT focus without human intervention is desirable to achieve a high degree of consistency and picture quality. In order to automate the focus adjustment process, we need a quantitative measure of focus, and the computation time of the measure must be performed in real time.

Since high frequency components determine dominantly the sharpness of objects in the image, conventional methods for focus (or defocus) measures are based on the energy of image gradients or point spread function (PSF) of edges. In gradient-based methods (Swain *et al.* 1994; Lee *et al.* 1995; Swain and Chen 1995; Fox *et al.* 1999), the  $3 \times 3$  Sobel operators are commonly used to detect edge and calculate the magnitude of gradients. The energy of image gradient is often defined as a focus measure whose value is supposed to be a maximum in the best-focused image. In PSF approaches (Pentland 1987; Hofeva 1994; Kim *et al.* 1998), the blurred edge is modeled as the result of convolving a perfectly focused image with a point spread function that is generally assumed to be a Gaussian distribution with

spatial parameter  $\sigma$ . The spatial parameter is associated to the radius of the blur circle, and is used as the focus measure. The estimation of the Gaussian parameter  $\sigma$  generally requires a complicated numerical optimization method (Lai and Fu 1992), and becomes impractical for on-line application. Also, many PSF-based blur estimation algorithms (Ens and Lawrence 1993; Subbarao and Surya 1994; Nayar and Nakagawa 1994) require two or more images obtained by changing focal length of the lens or diameter of the lens aperture. These involve relatively low mechanical movement of the camera and need specialized camera system whose parameter setting must be controlled precisely.

In recent years, Schechner *et al.* (2000) studied the problem of separating transparent layers that appear in semi-reflected scenes using a focus-based approach. They proposed a method for estimating the point spread functions. It is based on seeking the minimum Kullback distance of the mutual information between the recovered layers. Konnai and Hoshino (2001) performed DCT (Discrete Cosine Transformation) on captured images and the best-focused image is selected by monitoring the high frequency ratio of DCT. They show that the high frequency component of DCT increases when the image becomes sharp. Asif and Choi (2001) proposed a scheme for shape from focus. The method is based on representation of 3D focused image surface. The neural networks are trained to learn the shape of the focused image surface that maximizes the focus measure. Ziou and Deschenes (2001) presented an algorithm for measuring the difference in blur between two images. The algorithm is based on a local image decomposition technique using the Hermite polynomial basis. They show that any coefficient of the Hermite polynomial computed from the more blurred image is a function of the partial derivatives of the other image and the blur difference.

The gradient-based and PSF-based methods aforementioned are generally based on the local edge information in an image. Since edges are detected and processed in a pixel-by-pixel basis, focus measures of the conventional methods may result in significant amount of variation and require a large amount of computation time. For CRT adjustment application, the test pattern on the screen can be predetermined. Thus the focus measure can be evaluated based on the global area of the test pattern, rather than the local edge pixels, in the image so that the computation of focus magnitude can be robust and efficient. In this paper, we use the moment-preserving principle, which gives closed-form solution and is computationally fast, to quantify the degree of focus for a given test pattern in the image. In the CRT focus inspection, the monitor used in the study displays a predetermined white line pattern to a machine vision system. The area ratio of the line pattern with respect to its enveloped window of fixed size is then calculated using the moment-preserving method. A defocused screen will make the edge of a white line strip scattered and expand the area of the line strip accordingly. The best focus of a video screen under inspection can be obtained when the resultant area ratio is a minimum. The use of area ratio as a quantitative measure of focus is not only computationally fast but also physically meaningful to indicate the degree of change in defocus.

This paper is organized as follows: Section 2 describes the moment-preserving procedure for quantitative evaluation of focus. Section 3 presents the experimental results that show the efficacy of the proposed focus measure, and discusses the design of a best line pattern that will be sensitive to the change of varying focus voltage, and yet remain high repeatability with a given focus voltage. The paper is concluded in Section 4.

## 2. Quantitative measure of focus

For a test pattern that contains white objects in the black background on the CRT screen, the well-focused pattern shows sharp edges. The edges of white objects in the test pattern will be blurred, and the areas of the white target objects are then expanded outward when the amount of defocus increases. Figure 1(a) shows a focused “@” pattern, and Figure 1(b) presents a defocused version of the pattern. It can be seen from the figures that the white object region on the defocused screen is significantly larger than the one on the focused screen. The area ratio of the white target objects with respect to a given image size will get larger as the degree of defocus increases. Therefore, it can be used as a focus measure. In this study, we use a straightforward moment-preserving method to calculate the area ratio for quantitative evaluation of focus.

In the CRT focus inspection, a test pattern containing white objects in the black background is used for focus evaluation. Let  $f(x, y)$  be the gray level of a pixel at  $(x, y)$  in the sensor image that corresponds to the observed test pattern on the CRT screen. The test pattern that contains only object and background regions involves multiple gray levels in the sensed image. An ideal version of the image  $f(x, y)$  will consist of only two homogeneous regions, the white region (target objects) with a uniform gray level  $g_w$ , and the black region (the background) with a uniform gray level  $g_b$ . Denote  $p_w$  and  $p_b$  by the proportions of the object and background regions, respectively, in the ideal binary image. Note that  $g_w > g_b$ ,  $0 \leq p_w$ ,  $p_b \leq 1$  and  $p_w + p_b = 1$ . The first three moments of  $f(x, y)$  are given by

$$m_k = \frac{1}{M \times N} \sum_{y=0}^{N-1} \sum_{x=0}^{M-1} [f(x, y)]^k, \quad k = 1, 2, 3 \quad (1)$$

where  $M \times N$  is the image size of  $f(x, y)$ .

There are four unknown variables  $g_w$ ,  $g_b$ ,  $p_w$  and  $p_b$  that needed to be solved. By preserving the first three moments in both the sensed image  $f(x, y)$  and the ideal version of the image, we can obtain four equations as follows:

$$p_w \cdot g_w + p_b \cdot g_b = m_1 \quad (2a)$$

$$p_w \cdot g_w^2 + p_b \cdot g_b^2 = m_2 \quad (2b)$$

$$p_w \cdot g_w^3 + p_b \cdot g_b^3 = m_3 \quad (2c)$$

and

$$p_w + p_b = 1 \quad (2d)$$

There exists a closed-form solution (Tsai 1985) for the four unknown variables  $g_w$ ,  $g_b$ ,  $p_w$  and  $p_b$ , which are given by

$$g_w = \frac{1}{2} \left[ -c_1 + (c_1^2 - 4c_0)^{1/2} \right], \quad (3a)$$

$$g_b = \frac{1}{2} \left[ -c_1 - (c_1^2 - 4c_0)^{1/2} \right], \quad (3b)$$

$$p_b = \frac{\begin{vmatrix} 1 & 1 \\ m_1 & g_w \end{vmatrix}}{\begin{vmatrix} 1 & 1 \\ g_b & g_w \end{vmatrix}}, \quad (3c)$$

$$p_w = 1 - p_b \quad (3d)$$

where

$$c_0 = \frac{1}{(m_2 - m_1^2)} \begin{vmatrix} -m_2 & m_1 \\ -m_3 & m_2 \end{vmatrix}$$

$$c_1 = \frac{1}{(m_2 - m_1^2)} \begin{vmatrix} 1 & -m_2 \\ m_1 & -m_3 \end{vmatrix}$$

$g_w$  represents an ideal uniform gray value of the white target objects, and  $p_w$  is the corresponding proportion of the number of object pixels with respect to the total number of pixels in the given image. Therefore, the value of  $p_w$ ,  $0 \leq p_w \leq 1$ , gives the area ratio of the white object region in the sensed image. In Figure 1, the area ratio  $p_w$  of the focused pattern (Figure 1(a)) is 0.252, whereas the  $p_w$  value of the defocused pattern (Figure 1(b)) is increased to 0.331. For a given test pattern on the CRT screen, the best focus of the CRT will have the minimum area ratio. Any defocused screens will generate larger  $p_w$  values. In the conventional procedure of the focus adjustment, it is difficult to set the quantitative criteria for an acceptable focus. However, with the use of area ratio  $p_w$ , we can easily find the correct voltage that gives the best focus. The focus adjustment potentiometer can be tuned increasingly from low voltage to high voltage, and the corresponding  $p_w$  value as a function of focus voltage will generate a concave curve, where the valley of the curve (minimum  $p_w$  value) gives the correct focus voltage that results in the best picture sharpness.

### 3. Experimental results

In this section we present experimental results for evaluating the performance of the proposed focus measure, and discuss the design of a best test pattern for CRT focus adjustment. In our implementation, the algorithm is programmed in the VB language and executed on a personal computer with a Pentium III 500 MHz processor. The image size is 640 x 480 pixels with 256 gray levels. The camera with an 8.5 mm lens is set up so that the camera is 800 mm from the CRT screen. A test pattern (either a vertical or a horizontal line pattern) of 100 x 100 pixels in the sensed image corresponds to a physical inspection area of 12.5 x 12.5  $mm^2$  on the CRT screen.

The CRT resolution in the  $12.5 \times 12.5 \text{ mm}^2$  area is approximately  $85 \times 64$  pixels (i.e.,  $1024 \times 768$  of the whole CRT screen). In order to avoid the effect of inter-lacing, a slow shuttle speed of  $1/30$  second for the CCD camera and a refresh rate of 60 Hz for the CRT screen are used so that the inter-laced signal can be synchronized.

The color of a CRT screen is generated from the electron beams of the *R*, *G* and *B* phosphors. To prevent the effect of *RGB* convergence on focus measurement, only the color of green (i.e., a single *G* phosphor) instead of the white color (all three *R*, *G* and *B* phosphors are activated) is used to display the test pattern on the screen. The color CRT used for the experiment is a 17" computer monitor that has two separate focus adjustment potentiometers – one for static voltage that is used to adjust the horizontal focus, and another one for dynamic voltage that is used to adjust the vertical focus in the CRT manufacturing process. Therefore, we use two line patterns, one with vertical line strips for evaluating the horizontal focus, and the other one with horizontal line strips for evaluating the vertical focus. Each line pattern generated on the screen contains four line strips. The width of each line strip is 5 pixels, and the spacing between line strips is also 5 pixels on the CRT screen. Figures 2(a) and 2(b) show the vertical and horizontal line patterns used in the experiment.

Since no single setting of a given focus voltage will generate the same picture sharpness over the entire screen, the inspected area of the screen generates 72 sets of line patterns, which contain 36 vertical and 36 horizontal line patterns. For the camera setup aforementioned, the image from one CCD camera covers only a quarter of the CRT screen. In the corresponding sensor images from the four cameras that cover the whole CRT screen, the input images are divided into 72 subimages. The

focus measures in individual vertical and horizontal directions are then represented by the average area ratio  $\bar{p}_w$  from the 36 subimages. Figure 3 shows the picture that contains 36 vertical and 36 horizontal line patterns on the CRT screen. Since the proposed focus measure is computationally simple, computation time for 72  $p_w$  values (36 vertical and 36 horizontal line patterns) is only 0.1 second on a Pentium III-500 MHz personal computer.

In this experiment, the static focus voltage ranges from 6310 to 6670 volts in 30 volts increments, and the dynamic focus voltage varies from 6240 to 6600 volts, also in 30 volts increments. Figures 4 and 5 show the images of vertical and horizontal line patterns at various levels of focus voltage. The images from top to bottom (Figure 4) and the ones from left to right (Figure 5) are the results from low voltages to high voltages. It can be seen from Figures 4 and 5 that the picture sharpness is greatly improved when the correct focus voltage is selected. Table 1 summarizes the average area ratios  $\bar{p}_w(v)$  and  $\bar{p}_w(h)$  in respective vertical and horizontal directions at various levels of focus voltage. Figure 6 graphically presents the average area ratios as a function of focus voltage. Note that the resulting curves in Figure 6 are concave functions for both horizontal focus and vertical focus. The minimum value of area ratio indicates the correct focus voltage that generates the sharpest picture. The middle images in Figures 4 and 5 show the corresponding line patterns in the sensor images that use 6490 volts for horizontal focus, and 6390 volts for vertical focus. The focus measures  $p_w$  as a function of voltage for the experimental data in Table 1 can be well approximated by third-order regression models, and the R-square values of the fitting models are as high as 98.3% and 96.3% for horizontal focus and vertical focus, respectively.

We have also used the gradient-based method to evaluate the test images shown in Figures 4 and 5. The mean energies of image gradients for the vertical-line patterns from top to bottom in Figure 4 are 156.1, 157.7, 148.7, 144.6 and 146.0, respectively. Also, the mean energies of image gradients for the horizontal-line patterns from left to right in Figure 5 are 157.0, 156.9, 156.8, 156.1 and 155.6. The results reveal that the focus measures given by the energy of image gradients are not sensitive to the change of focus voltage, and the maxima are not responsive to the best-focused images.

In this study, we have also conducted an experiment to evaluate the effect of different line patterns on the performance of the proposed focus measure. The line patterns are constructed by varying the line widths and spacings from 4 to 7 pixels in 1-pixel increment. Figure 7 shows some line patterns with different combinations of line widths and spacings used in the experiment. The line widths or spacings smaller than 4 pixels are not considered in the experiment because the current camera setup cannot provide sufficient image resolution for the test. The measure of quality is chosen on the basis of how a line pattern well separates the average area ratio  $\bar{p}_w$  between different focus voltages and keeps the samples of individual focus voltage close together. For horizontal focus measurement, the static voltage is adjusted from 6310 to 6670 volts in 30 volts increments. This generates a total of 13 voltage sets. For each individual static voltage, 30 samples of the average area ratios  $\bar{p}_w$  are collected. The selection criterion of a best line pattern is achieved by comparing inter-set variance between different levels of focus voltage and intra-set variance of the samples in the same voltage set, i.e.,

$$Q_f = \frac{\sigma_b^2}{\sigma_w^2}$$

where  $\sigma_b^2$  is the variance of  $\bar{p}_w$  between voltage sets, and  $\sigma_w^2$  is the variance of  $\bar{p}_w$  within a voltage set.  $Q_f$  defines the variance ratio between  $\sigma_b^2$  and  $\sigma_w^2$ . A best line pattern should have the maximum interset variance  $\sigma_b^2$  and minimum intraset variance  $\sigma_w^2$  so that the focus measure can be sensitively responsive to the change of focus voltage while maintaining good repeatability and stability of the evaluated  $\bar{p}_w$  values.

Table 2 summarizes the interset and intraset variances and the variance ratio  $Q_f$  for the line patterns with different combinations of line widths and spacings. As shown in Table 2, the intraset variance is generally around  $10^{-8}$ . This indicates that the proposed focus measure based on the global area instead of the local edges of an object pattern is very stable. The variance ratio  $Q_f$  is extremely large for all line patterns. Line patterns with narrow line widths and spacings generally outperform those with broad line widths and spacings. The line pattern with line width and spacing of 4 pixels yields the maximum variance ratio  $Q_f$ . The same result is also obtained for the horizontal line patterns that are used for measuring the vertical focus. The experimental result is consistent with ordinary focus measures since fine details (narrow line width) are affected by blur more strongly than coarse details (broad line width).

#### 4. Conclusions

In this paper we have used the moment-preserving method for quantitative

evaluation of focus performance. The focus measure is represented by the area ratio of the line pattern with respect to a given image size. Since the area ratio is evaluated from the global region rather than from the local edges of the test pattern, the resultant value is sensitively responsive to the minor change of focus voltage while it can maintain excellent repeatability for individual focus voltages.

The proposed moment preserving method is straightforward and gives closed-form solution of the focus measure. Computation time for 72 line patterns on a typical personal computer is less than 0.1 seconds. Thus one-line, real-time application of focus adjustment can be realized with the proposed method. The proposed method in this study basically aims at CRT focus measurement. It can be also extended for LCD projectors and other video display devices.

## References

- Anttila P, Tolmunen T (1997) A novel focus meter. *IEEE Trans. Consumer Electronics* 43: 807-812.
- Asif M, Choi TS (2001) Shape from focus using multiplayer feedforward neural networks. *IEEE Trans. Image Processing* 10: 1670-1675.
- Ens J, Lawrence P (1993) An investigation of methods for determining depth from focus. *IEEE Trans. Pattern Anal. Machine Intell.* 15: 97-107.
- Fox S, Silver RM, Kornegay E, Dagenais M (1999) Focus and edge detection algorithms and their relevance to the development of an optical overlay calibration standard. In: *Proc. of SPIE – The International Society for Optical Engineering* 3677, 95-106.
- Hofeva LF (1994) Range estimation from camera blur by regularized adaptive identification. *Int. J. Pattern Recog. Artificial Intell.* 8:1273-1300.
- Kim SK, Park SR, Paik JK (1998) Simultaneous out-of-focus blur estimation and restoration for digital auto-focusing system. *IEEE Trans. Consumer Electronics* 44: 1071-1075.
- Konnai K, Hoshino Y (2001) Method of capturing image of object passing through focus area. In: *Proc. of SPIE – The International Society for Optical Engineering* 4308, pp 86-94.
- Lai SH, Fu CW (1992) A generalized depth estimation algorithm with a single image. *IEEE Trans. Pattern Anal. Machine Intell.* 14: 405-411.
- Lee JH, Kim KS, Nam BD (1995) Implementation of a passive automatic focusing algorithm for digital still camera. *IEEE Trans. Consumer Electronics* 41: 449-454.
- Nayar SK, Nakagawa Y (1994) Shape from focus. *IEEE Trans. Pattern Anal. Machine Intell.* 16: 824-831.
- Pentland AP (1987) A new sense for depth of field. *IEEE Trans. Pattern Anal. Machine Intell.* PAMI-9: 523-531.
- Schechner YY, Kiryati N, Basri R (2000) Separation of transparent layers using focus. *Int. J. Computer Vision* 39: 25-39.

Subbarao M, Surya G (1994) Depth from defocus: a spatial domain approach. *Int. J. Computer Vision* 13: 271-294.

Swain C, Chen T (1995) Defocus-based image segmentation. *Acoustics, Speech and Signal Processing* 4: 2403-2406.

Swain C, Peters A, Kawamura K (1994) Depth estimation from image defocus using fuzzy logic. *Fuzzy Systems* 1: 94-99.

Tsai WH (1985) Moment-preserving thresholding: a new approach. *Computer Vision Graphics Image Process.* 29: 377-393.

Ziou D, Deschenes F (2001) Depth from defocus estimation in spatial domain. *Computer Vision and Image Understanding* 81: 143-165.

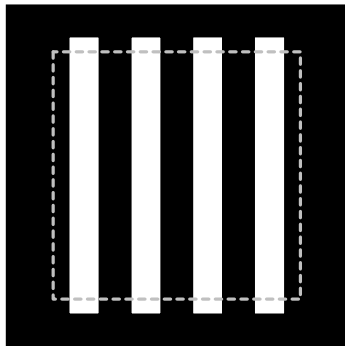


(a)

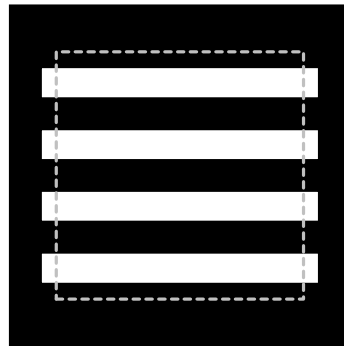


(b)

Figure 1. (a) A focused image that contains nine “@”s; (b) a defocused version of (a).



(a)



(b)

Figure 2. (a) The vertical line pattern used for evaluating the horizontal focus; (b) the horizontal line pattern used for evaluating the vertical focus.

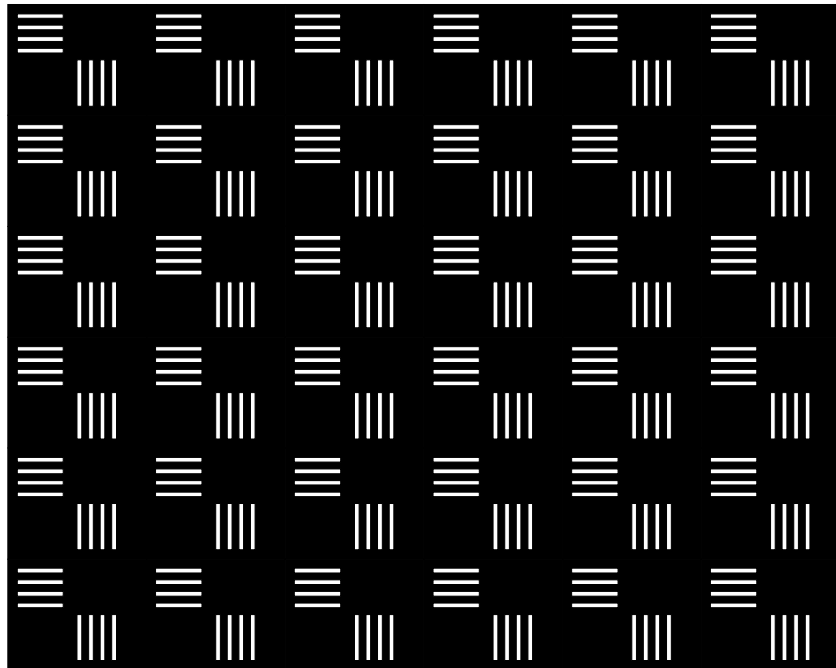


Figure 3. An inspected screen area that contains 36 vertical and 36 horizontal line patterns.

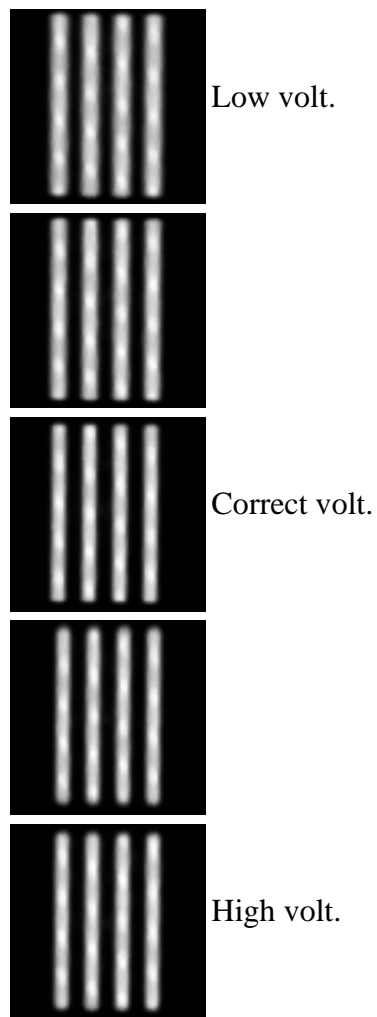


Figure 4. The images of vertical line patterns at various levels of static focus voltage.

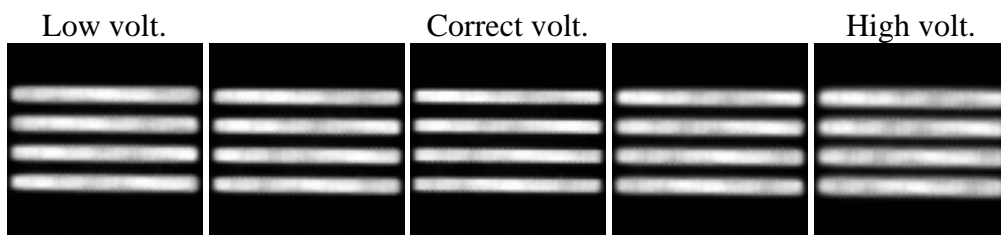


Figure 5. The images of horizontal line patterns at various levels of dynamic focus voltage.

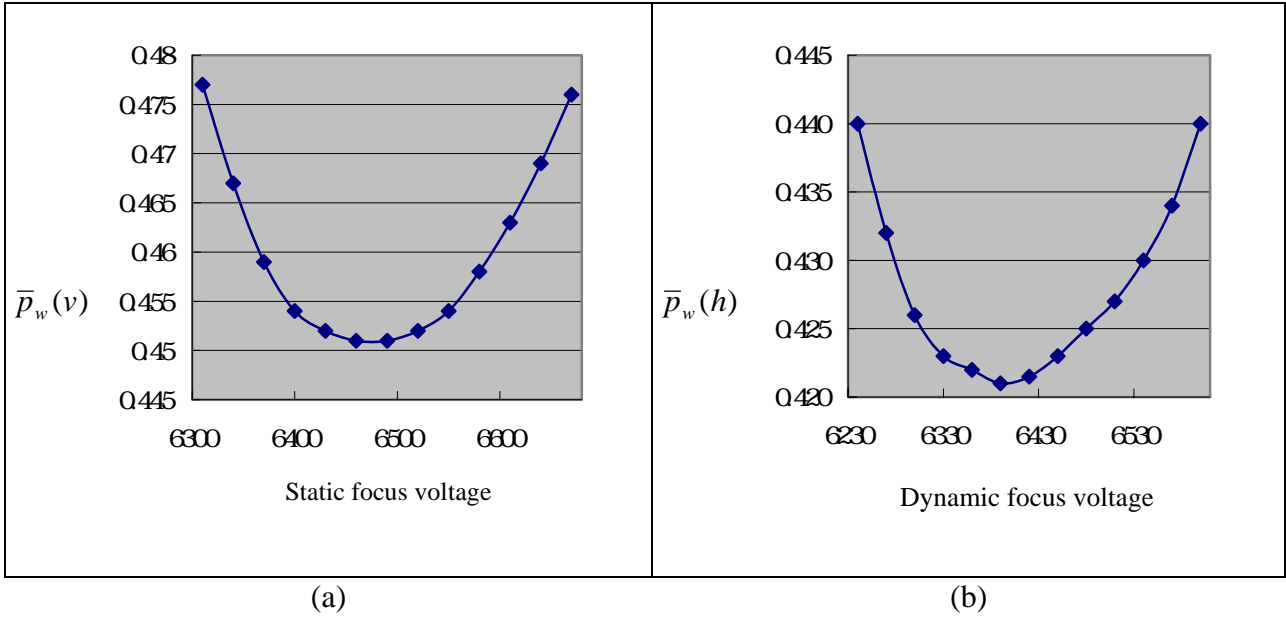


Figure 6. The average area ratios  $\bar{p}_w$  as a function of focus voltage: (a) the resulting curve for horizontal focus; (b) the resulting curve for vertical focus.

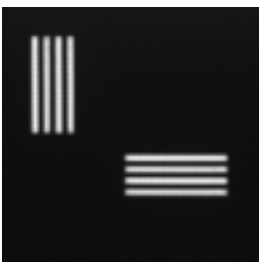
Line width (pixel)	Line spacing (pixel)	Line pattern	Line width (pixel)	Line spacing (pixel)	Line pattern
4	4		6	3	
4	5		6	4	
4	6		6	5	
5	3		7	3	
5	4		7	4	
5	5		7	5	

Figure 7. Line patterns with various line widths and spacings.

Table 1. The statistics of  $\bar{p}_w$  at various levels of voltage for horizontal focus and vertical focus.

Static focus voltage (volt)	6310	6340	6370	6400	6430	6460	6490	6520	6550	6580	6610	6640	6670
$\bar{p}_w(v)$	0.477	0.467	0.459	0.454	0.452	0.451	0.451	0.452	0.454	0.458	0.463	0.469	0.476
Dynamic focus voltage (volt)	6240	6270	6300	6330	6360	6390	6420	6450	6480	6510	6540	6570	6600
$\bar{p}_w(h)$	0.440	0.432	0.426	0.423	0.422	0.421	0.4215	0.423	0.425	0.427	0.430	0.434	0.440

Table 2. The interset and intraset variances of  $\bar{p}_w(v)$  for line patterns with various line widths and spacings.

Average area ratios $\bar{p}_w$ from static focus voltages				
Line width (pixel)	Line spacing (pixel)	Interset variance $\sigma_b^2$	Intraset variance $\sigma_w^2$	Variance ratio $Q_f = \sigma_b^2 / \sigma_w^2$
4	4	2.3E-3	1.7E-8	1.4E+5
4	5	4.0E-3	3.8E-8	1.0E+5
4	6	2.7E-3	2.7E-8	9.8E+4
4	7	1.5E-3	1.6E-8	9.6E+4
5	4	3.2E-3	6.1E-8	5.3E+4
5	5	3.2E-3	5.3E-8	6.1E+4
5	6	1.8E-3	4.5E-8	4.0E+4
5	7	7.6E-4	3.0E-8	2.5E+4
6	4	2.9E-3	9.4E-8	3.1E+4
6	5	2.1E-3	8.3E-8	2.5E+4
6	6	6.0E-4	4.7E-8	1.3E+4
6	7	4.7E-4	6.8E-8	7.0E+3
7	4	2.6E-3	9.8E-8	2.6E+4
7	5	1.1E-3	9.5E-8	1.1E+4
7	6	2.1E-4	5.4E-8	3.9E+3
7	7	4.3E-4	1.2E-6	3.7E+2